Control of 3 DOF Quadrotor Model

Tae Soo Kim, Karl Stol, Vojislav Kecman
Departement of Mechanical Engineering
The University of Auckland
Auckland, New Zealand
tkim020@ec.auckland.ac.nz k.stol@auckland.ac.nz v.kecman@auckland.ac.nz

Abstract – The modeling and control of 3 Degrees-of-Freedom (DOF) four-rotor rotorcraft is presented in this paper. Optimal control (LQR), LQR with gain scheduling, feedback linearization and sliding-mode control are simulated and tested on an experimental rig. The performance of the individual controllers are compared and discussed. Our simulation showed Sliding Mode Control (SMC) returned the best performance with the fastest state regulation while LQR with gain scheduling produced relatively good performance with less total control effort.

I. INTRODUCTION

Unmanned aerial vehicles (UAVs) comprise various types of aircrafts such as conventional fixed-wing aircraft, helicopter, blimps and airships. Among these, helicopters are classified as Planar Vertical Take Off and Landing (PVTOL) aircraft by which it means that unlike a fixed-wing aircraft, it can take off and land in a limited space, hover in the air, and move sideways and backwards. This superior maneuverability allows performing important roles in many areas, where conventional aircraft could not achieve. The type of their useful work includes: dangerous applications such as in a war, victim rescue and volcano monitoring, where other types of vehicle are inaccessible, commercial application such as film making, and agricultural applications, farm monitoring and spreading chemicals. The demand for UAVs keep increasing. Unfortunately these exclusive maneuverability advantages give a big complexity and instability in its dynamics, hence making it hard to control. The development of a UAV is challenging, and it is an emerging area in nonlinear control study among researchers.

A few researchers focused on applying various control techniques to a quadrotor. Lozano et al. [1] approached global stabilization of PVTOL vehicle using Lyapunov analysis, designing a simple nonlinear controller by analysing boundness and convergence of each state. Bouabdallah et al. [2,3,4] have built a micro VTOL autonomous robot, ‘OS4’. OS4 was a three DOF model controlling only rotations. Lyapunov theorem was used for controller design. Later they have explored the application of two different techniques, PID and linear quadratic (LQ) to OS4. OS4 at near-hover condition was tested, neglecting gyroscopic effects from the rigid body and propeller rotation, i.e. removing all cross couplings.

Design and tuning are important aspect in UAV design. Pounds et al. [5] worked with blade designs to optimize the thrust generation and dynamic stability. Airfoil design and material properties of blade were studied and the flapping behaviour of a blade were analysed by adapting an existing mathematical model.

At the University of Auckland, a number of undergraduate projects have been undertaken to study the control of helicopter models. In 2003, R. Murphy and T. Hay designed and controlled a rig that replicated pitching motion of a helicopter using a PID controller. In 2004 W. Zhao and T. Kim worked on the single DOF altitude control of a helicopter. Also in the same year, A. Stojanovic constructed a 2DOF helicopter model controlling pitch and yaw using a PLC. In 2006, D. Campbell and L. D'Souza, had attempted to create a free-flying semi-autonomous quadrotor helicopter. With a micro controller programmed with PD controller, the quadrotor was able to hover in the air for a few seconds, yet it was not stable enough for a free flight. Limitations of classical control on a complex dynamic plant were observed.

In this research we aimed to develop control algorithms to stabilize an unstable quadrotor plant and implement this on an experimental rig. A few control techniques are simulated and their performances are compared.

II. MODELLING OF A QUADROTOR

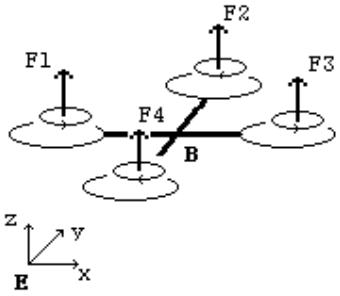

ϕ: pitch angle – rotation about y-axis

θ: roll angle – rotation about x-axis

ψ: yaw angle – rotation about z-axis

E: the inertial frame

B: body fixed frame

Figure 1 Quadrotor configuration

The Quadrotor in Figure 1 can be modeled as a 6 DOF rigid body; three translations, movement along X, Y and Z coordinate, and three rotations, pitch, roll and yaw, which are rotations about X, Y and Z axis respectively. The quadrotor is an underactuated system; there are fewer individual inputs than the DOF to be controlled. Some states are controlled through other states. The movement along Y axis is controlled by the pitch angle ϕ. Increasing the force F4 relative to F2, while the sum of all four thrust balances the weight mg results in rotation in ϕ, induces the movement of the body along Y axis, the axis in body fixed frame B in Figure 1. In a similar way, the movement along X axis is controlled by the roll angle θ. Movement along vertical Z axis occurs by increasing the thrusts from all four rotors so that the collective thrust exceeds the weight of the rig. While doing this, thrust from each rotor must balance the thrust from the opposite rotor. Rotors 1 & 3 rotate clockwise direction and rotors 2 & 4 rotate anticlockwise direction to counter-balance the gyroscopic moments causing the rigid body rotation about Z axis.

Prior to simulation, a mathematical model for quadrotor is derived. For derivation, notation from [2] is followed. Dynamic model of a quadrotor is expressed as:

$$\ddot{\phi} = \dot{\theta}\dot{\psi}\left(\frac{I_y - I_z}{I_x}\right) - \frac{J_p}{I_x}\dot{\theta}(\Omega_2 + \Omega_4 - \Omega_1 - \Omega_3) + \frac{l}{I_x}b(\Omega_4^2 - \Omega_2^2) \quad (1)$$

$$\ddot{\theta} = \dot{\phi}\dot{\psi}\left(\frac{I_z - I_x}{I_y}\right) + \frac{J_p}{I_y}\dot{\phi}(\Omega_2 + \Omega_4 - \Omega_1 - \Omega_3) + \frac{l}{I_y}b(\Omega_3^2 - \Omega_1^2) \quad (2)$$

I: body moment of inertia

J_p: propeller inertia

l: lever

Ω: angular speed of rotor

$$\ddot{\psi} = \dot{\theta}\,\dot{\phi}\left(\frac{I_x - I_y}{I_z}\right) + \frac{I}{I_z} d\,(\Omega_2^2 + \Omega_4^2 - \Omega_1^2 - \Omega_3^2) \qquad (3)$$

b: thrust coefficient

d: drag coefficent

The assumptions for this model are:

- The body is rigid and is symmetrical.
- The centre of mass and the body fixed frame origin coincides.
- The propellers are rigid. i.e. no blade flapping occurs.

As the equations show there is coupling present between rotational speeds of the body.

III. OPENLOOP BEHAVIOUR

The quadrotor plant has an equilibrium point when all three angles are zero, thrusts from four rotors are equal and the collective thrust balances the weight. However in practice disturbances due to wind, vibrations from motor and imbalance in the structure do not allow the plant to remain stable at the equilibrium point. To observe the stability characteristics of the quadrotor, an open-loop simulation was performed in Simulink. The simulation conditions are:

- Initial pitch, yaw and roll angles are set to zero.
- Sum of the thrusts from four rotors equal to the weight of quadrotor where three thrusts are equal and thrust from one is varied by 5%.
- The actuator dynamics are not modelled.

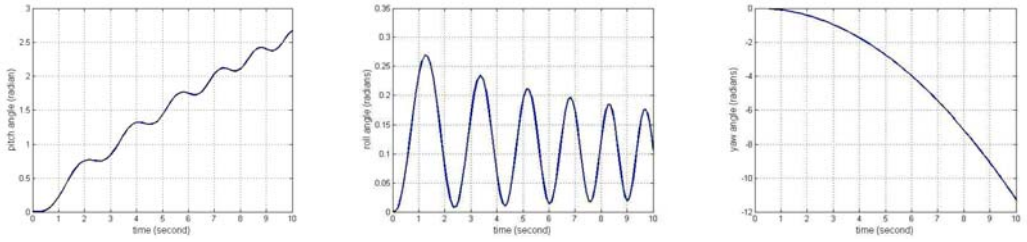

Figure 2 Open loop response of quadrotor in pitch, roll and yaw.

As shown in the open loop response in Figure 2, an uncontrolled quadrotor is unstable. Thus, it requires a controller to stabilize the system.

IV. EXPERIMENTAL SETUPS

An experimental rig, replicating the attitude of a quadrotor is designed to apply control algorithm. The design specification for the rig is:

- A 3 DOF model must fully replicate the rotational motion of a quadrotor. The translational DOFs are removed.
- The centre of mass of the rig must coincide with the centres of three rotations. This is to ensure the resulting motions are pure rotations.
- The operating range for pitch and roll are ± 40 degrees and ± 180 degrees for the yaw.

Three optical incremental encoders, HP HEDS5700, are chosen for measuring individual rotation. DSpace control board DS1104 is used for data acquisition and produce PWM control signal to the motors along with Simulink and Control Desk. DS1104 supports two incremental encoder inputs and four PWM pulse generation. The extra encoder is interfaced through digital bit I/O port. Motors, gears, propellers

and carbon fibre arms are from a commercial quadrotor design, the Dranganfly V [6].

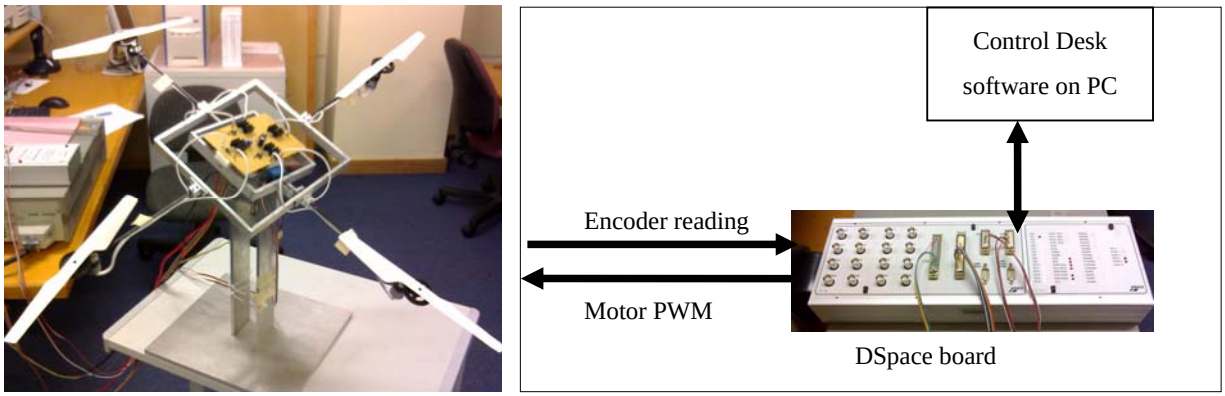

Figure 3 Quadrotor Experimental Rig

V. CONTROL DESIGN

A. Optimal Control (LQR)

Linearization of the nonlinear quadrotor plant is the first step for deriving a linear control law. The plant is linearized about an equilibrium point at which the three orientation angles ϕ, θ, ψ and its velocities $\dot{\phi}$, $\dot{\theta}$, $\dot{\psi}$ are zero and the angular speed of four rotors are equal. The linearization results:

$$\begin{bmatrix} \Delta\dot{\phi} \\ \Delta\dot{\theta} \\ \Delta\dot{\psi} \\ \Delta\ddot{\phi} \\ \Delta\ddot{\theta} \\ \Delta\ddot{\psi} \end{bmatrix} = \begin{bmatrix} 0 & 0 & 0 & 1 & 0 & 0 \\ 0 & 0 & 0 & 0 & 1 & 0 \\ 0 & 0 & 0 & 0 & 0 & 1 \\ 0 & 0 & 0 & 0 & 0 & 0 \\ 0 & 0 & 0 & 0 & 0 & 0 \\ 0 & 0 & 0 & 0 & 0 & 0 \end{bmatrix} \begin{bmatrix} \Delta\phi \\ \Delta\theta \\ \Delta\psi \\ \Delta\dot{\phi} \\ \Delta\dot{\theta} \\ \Delta\dot{\psi} \end{bmatrix} + \begin{bmatrix} 0 & 0 & 0 & 0 \\ 0 & 0 & 0 & 0 \\ 0 & 0 & 0 & 0 \\ 0 & -2b\frac{l}{I_x}\Omega_{ss} & 0 & 2b\frac{l}{I_x}\Omega_{ss} \\ -2b\frac{l}{I_y}\Omega_{ss} & 0 & 2b\frac{l}{I_y}\Omega_{ss} & 0 \\ -2d\frac{l}{I_z}\Omega_{ss} & 2d\frac{l}{I_z}\Omega_{ss} & -2d\frac{l}{I_z}\Omega_{ss} & 2d\frac{l}{I_z}\Omega_{ss} \end{bmatrix} \begin{bmatrix} \Delta\Omega_1 \\ \Delta\Omega_2 \\ \Delta\Omega_3 \\ \Delta\Omega_4 \end{bmatrix} \tag{4}$$

With appropriate choice of Q and R matrices in cost function, $J = \int_0^\infty (\underline{x}^T Q \underline{x} + \underline{u}^T R \underline{u}) dt$, the control gain K in $\underline{u} = -K\underline{x}$ is obtained using Matlab.

B. LQR with Gain Scheduling

Small sphere approximating approach for linearization is implemented with gain scheduling. Linearization is performed continuously to re-linearize about every operating point along the state trajectory. The resulting matrix form of the equations is:

$$\begin{bmatrix} \Delta\dot{\phi} \\ \Delta\dot{\theta} \\ \Delta\dot{\psi} \\ \Delta\ddot{\phi} \\ \Delta\ddot{\theta} \\ \Delta\ddot{\psi} \end{bmatrix} = \begin{bmatrix} 0 & 0 & 0 & 1 & 0 & 0 \\ 0 & 0 & 0 & 0 & 1 & 0 \\ 0 & 0 & 0 & 0 & 0 & 1 \\ 0 & 0 & 0 & 0 & I_1\bar{\dot{\psi}} - I_4\bar{\Omega} & I_1\bar{\dot{\theta}} \\ 0 & 0 & 0 & I_2\bar{\dot{\psi}} + I_5\bar{\Omega} & 0 & I_2\bar{\dot{\phi}} \\ 0 & 0 & 0 & I_3\bar{\dot{\theta}} & I_3\bar{\dot{\phi}} & 0 \end{bmatrix} \begin{bmatrix} \Delta\phi \\ \Delta\theta \\ \Delta\psi \\ \Delta\dot{\phi} \\ \Delta\dot{\theta} \\ \Delta\dot{\psi} \end{bmatrix} + \begin{bmatrix} 0 & 0 & 0 & 0 \\ 0 & 0 & 0 & 0 \\ 0 & 0 & 0 & 0 \\ I_4\bar{\dot{\theta}} & -(I_4\bar{\dot{\theta}} + 2bI_6\bar{\Omega}_2) & I_4\bar{\dot{\theta}} & -I_4\bar{\dot{\theta}} + 2bI_6\bar{\Omega}_4 \\ -(I_5\bar{\dot{\phi}} + 2bI_7\bar{\Omega}_1) & I_5\bar{\dot{\phi}} & -I_5\bar{\dot{\phi}} + 2bI_7\bar{\Omega}_3 & I_5\bar{\dot{\phi}} \\ -2dI_8\bar{\Omega}_1 & 2dI_8\bar{\Omega}_2 & 2dI_8\bar{\Omega}_3 & -2dI_8\bar{\Omega}_4 \end{bmatrix} \begin{bmatrix} \Delta\Omega_1 \\ \Delta\Omega_2 \\ \Delta\Omega_3 \\ \Delta\Omega_4 \end{bmatrix} \tag{5}$$

where the moments of inertia are defined by:

$$I_1 = \frac{I_y - I_z}{I_x},\ I_2 = \frac{I_z - I_x}{I_y},\ I_3 = \frac{I_x - I_y}{I_z},\ I_4 = \frac{J_p}{I_x},\ I_5 = \frac{J_p}{I_y},\ I_6 = \frac{1}{I_x},\ I_7 = \frac{1}{I_y},\ I_8 = \frac{1}{I_z} \tag{6}$$

This is more accurate linearization of the plant, but recalculating the state matrix, input matrix and control gain *K* every step is computationally expensive. The control law becomes $\underline{u} = -K(t)\underline{x}$ where *K(t)* is time-varying control gain matrix.

C. Feedback Linearization

Using feedback linearization, nonlinear terms are canceled out by the control input. The derived control inputs are:

$$U_1 = \frac{I_x}{l}\left(-\dot{\theta}\dot{\psi}\left(\frac{I_y - I_z}{I_x}\right) + \frac{J_p}{I_x}\dot{\theta}(\Omega_2 + \Omega_4 - \Omega_1 - \Omega_3) - k_1 x\right) \tag{7}$$

$$U_2 = \frac{I_y}{l}\left(-\dot{\phi}\dot{\psi}\left(\frac{I_z - I_x}{I_y}\right) - \frac{J_p}{I_y}\dot{\phi}(\Omega_2 + \Omega_4 - \Omega_1 - \Omega_3) - k_2 x\right) \tag{8}$$

$$U_3 = \frac{I_z}{l}\left(-\dot{\theta}\dot{\phi}\left(\frac{I_x - I_y}{I_z}\right) - k_3 x\right) \tag{9}$$

where

$$U_1 = F_4 - F_2,\ U_2 = F_3 - F_1,\ U_3 = \tfrac{d}{b}(F_2 + F_4 - F_1 - F_3) \tag{10}$$

Equation 10 can be resolved into individual forces using pseudo inversion.

D. Sliding Mode Control

The Following sliding mode controller is developed to drive all the states to zero. The terms in the first bracket of Equations 11 through 13 cancel out the nonlinearities while the following term with *sign* switches control input to keep the system in a stable manifold [7].

$$U_1 = -\frac{I_x}{l}\left(\dot{\theta}\dot{\psi}\left(\frac{I_y - I_z}{I_x}\right) - \frac{J_p}{I_x}\dot{\theta}(\Omega_2 + \Omega_4 - \Omega_1 - \Omega_3) + \alpha_1\dot{\phi}\right) - K_1 sign(\dot{\phi} + \alpha_1\phi) \tag{11}$$

$$U_2 = -\frac{I_y}{l}\left(\dot{\phi}\dot{\psi}\left(\frac{I_z - I_x}{I_y}\right) + \frac{J_p}{I_y}\dot{\phi}(\Omega_2 + \Omega_4 - \Omega_1 - \Omega_3) + \alpha_2\dot{\theta}\right) - K_2 sign(\dot{\theta} + \alpha_2\theta) \tag{12}$$

$$U_3 = -\frac{I_z}{l}\left(\dot{\theta}\dot{\phi}\left(\frac{I_x - I_y}{I_z}\right) + \alpha_3\dot{\psi}\right) - K_3 sign\ (\dot{\psi} + \alpha_3\psi) \tag{13}$$

VI. SIMULATIONS

Simulations were run in Simulink for all four previously derived controllers. The controllers are set to regulate all states. The initial conditions are: $\phi = 0.5rad$, $\theta = 0.3rad$, $\varphi = -0.2rad$. The simulations are run for 50 seconds. Control parameters for each controller are tuned to produce similar control effort in given period of time.

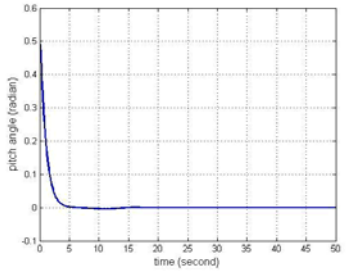

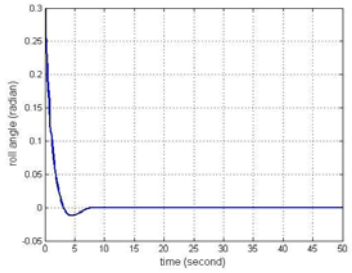

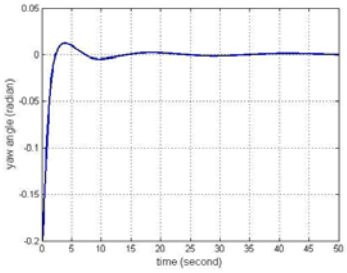

Figure 4 Simulation result for closed loop response

Figure 4 shows the simulation result for LQR, LQR with gain scheduling and feedback linearization. The three controllers showed almost equivalent results in the graph. Sliding mode control has a much shorter settling time. Its response is shown in Figure 5.

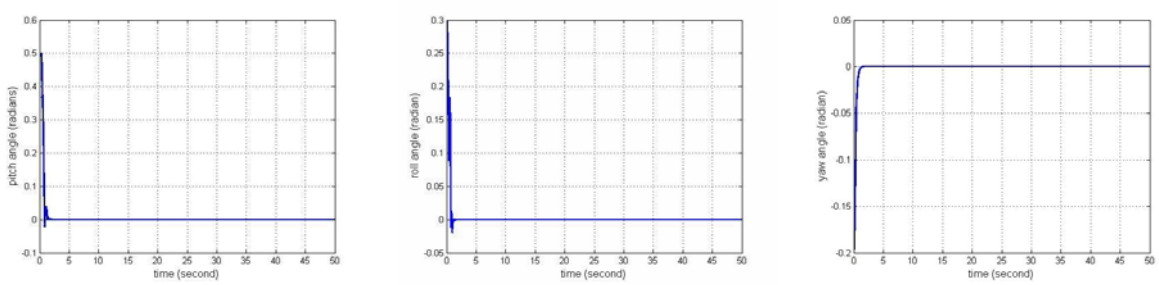

Figure 5 Simulation result for sliding mode controller

For numerical comparisons the performance index ITSE (Integral of Time multiplied by the Square of Error) is used with total control effort. ITSE is given by:

$$ITSE = \int_0^T te^2(t)dt \tag{14}$$

	ϕ	θ	φ	$\sum errors$	$\sum \lvert u(t) \rvert$
LQR	0.7226	0.2314	0.1288	1.0441	975.7009
Gain Schedule	0.5249	0.2321	0.1431	0.8571	978.9849
Feedback Lin.	0.6969	0.2171	0.1596	1.0258	978.7780
SMC	0.3344	0.0585	0.0171	0.4049	986.8826

Table 1 Comparison of controller performances

Table 1 shows the performance comparison of the four different control techniques. Yaw angle φ is regarded less important than the other two angles. To reflect this, a factor of 0.7 is multiplied to error for yaw angle. With similar control effort, the sliding mode controller returned the best simulation result. LQR with gain scheduling showed significantly better result than feedback linearization.

VII. EXPERIMENTAL RESULTS

The quadrotor model is currently undergoing a gain tuning stage. The simulation results will be tested on the experimental rig for real-time result and further comparison is to be done.

VIII. CONCLUSIONS

In this paper, four different control techniques; LQR, LQR with gain scheduling, feedback linearization and sliding mode control were derived and simulated. Comparing under ITSE criteria, sliding mode control produced the best result with the most rapid state regulation. While LQR with gain scheduling showed a relatively good performance compared to standard LQR and feedback linearization.

For more precise simulation, actuator dynamics can be incorporated into the model. A better approximation of inertia would allow better control performance on the real plant. Optical encoders are not suitable for measuring orientation angles for a free flying quadrotor. Our experimental rig can be further improved in

the future by reducing the weight and using other sensor combination for a complete 6 DOF free flying quadrotor.

REFERENCES

1. R. Lozano, P. Castillo, A. Dzul. “Global stabilization of the PVTOL: real-time application to a mini-aircraft”. Int. Journal of Control, Vol. 77, Number 8, pp 735-740, May 2004.

2. Bouabdallah, S., Noth, A. and Siegwart, R. (2004) PID vs LQ Control Techniques Applied to an Indoor Micro Quadrotor. In Proceedings of the IEEE International Conference on Intelligent Robots and Systems, Sendai, Japan, 2004.

3. Bouabdallah, S., Murrieri, P. and Siegwart, R. (2004) Design and Control of an Indoor Micro Quadrotor. In Proceedings of International Conference on Robotics and Automation, New Orleans, USA, 2004.

4. Bouabdallah, S. and Siegwart, R. (2005) Backstepping and Sliding-mode Techniques Applied to an Indoor Micro Quadrotor. In Proceedings of IEEE International Conference on Robotics and Automation, Barcelona, 2005.

5. Pounds, P. et al. (2004) Towards Dynamically-Favourable Quad-Rotor Aerial Robots. In Proc. Australian Conf. Robotics and Automation, Canberra, December 2004.

6. Draganfly Inovations Inc. Draganflyer Supplier. http://www.rctoys.com

7. Khalil, H.K.Nonlinear Systems, third edition, Prentice Hall, 2002.